

THE OXIDATION OF ETHANOL ON Cu(110) AND Ag(110) CATALYSTS

Israel E. WACHS and Robert J. MADIX

*Department of Chemical Engineering, Stanford University,
Stanford, California 94305, USA*

Received 19 October 1977

Revised manuscript received 16 December 1977

The oxidation of ethanol was studied on Cu(110) and Ag(110) single crystals by temperature programmed reaction spectroscopy. The single crystal surfaces were preoxidized with $^{18}\text{O}_2$, and deuterated ethanol, $\text{CH}_3\text{CH}_2\text{OD}$, was used to distinguish the hydroxyl hydrogen from the ethyl hydrogens. The ability of both surfaces to dissociatively chemisorb ethanol was greatly enhanced by surface oxygen. $\text{CH}_3\text{CH}_2\text{OD}$ was selectively oxidized upon adsorption at 180 K to adsorbed $\text{CH}_3\text{CH}_2\text{O}$ and D_2^{18}O . The Ag(110) surface was more active than the Cu(110) surface for the dehydrogenation of ethoxide to acetaldehyde and hydrogen. The recombination of surface hydrogen with ethoxide to yield $\text{CH}_3\text{CH}_2\text{OH}$ was also observed. Following high exposures of ethanol the surface intermediate $\text{CH}_3\text{CH}_2\text{OD}_2$ was produced upon adsorption at 180 K from the interaction of two $\text{CH}_3\text{CH}_2\text{OD}$ molecules, and this surface complex subsequently decomposed to C_2H_4 , D_2O and hydrogen. The present results for the oxidation of ethanol are compared to the previous investigations of methanol oxidation on Cu(110) and Ag(110).

1. Introduction

The catalytic oxidation of alcohols to aldehydes or ketones has been known for many years [1]. Methanol is oxidized to formaldehyde over silver or copper catalysts. With silver a rich mixture of methanol and air is employed and the catalyst temperature is 600–650°C. Conversions are upwards of 90% per pass, with yields of 80–90+% formaldehyde based on the methanol converted. With copper catalysts slightly higher reaction temperatures are utilized, 700–750°C [2]. Ethanol and air passed over silver catalysts at 550–570°C give 50–55% conversion per pass to acetaldehyde with an 85% yield. This process is also operated with a rich mixture of ethanol and air, although it is rarely used commercially because there are more economical ways of making acetaldehyde. Isopropanol gives acetone, and other higher alcohols also react over silver and copper catalysts, but catalytic dehydrogenation is ordinarily used instead of oxidation.

The catalytic dehydrogenation of primary and secondary alcohols also yields aldehydes or ketones [3]. Ethanol gives acetaldehyde; isopropanol gives acetone; sec-

butyl alcohol gives methyl ethyl ketone; etc. Methanol is usually *oxidized* to formaldehyde since dehydrogenation gives carbon monoxide plus hydrogen. The most widely used catalysts for dehydrogenation of alcohols are based on metallic copper, and reaction conditions are 250–400°C and atmospheric pressure. The reaction is endothermic and conversion is rarely over 50% per pass. Silver catalysts are also effective for dehydrogenation but rarely justify the incremental cost.

The interaction of ethanol with oxygen-free and partially oxidized (110) oriented single crystals of copper and silver was studied under ultrahigh vacuum conditions with the modern tools of surface science. The method of temperature programmed reaction spectroscopy (TPRS) was employed [4]. The purpose of this study was (i) to compare the interaction of ethanol on copper (110) with silver (110) and (ii) to compare the present results with the previous investigations of methanol on copper (110) [5] and silver (110) [6].

The reader should note that there are several basic concepts involved in interpreting mechanistic patterns from temperature programmed surface reaction studies. The most important of these is that reaction products evolved with identical flash peaks originate from the same rate-limiting step. This deduction follows from the equation for product evolution which takes the form $R = R(T_s, C_i)$ where the rate of product evolution, R , is a sensitive function of the surface temperature, T_s , and the concentration of adsorbed species, C_i . It has been well demonstrated that flash desorption methods are sensitive to binding energy changes of less than 0.1 kcal/gmole (5 meV). For the sake of mechanistic analysis it is therefore quite reasonable to assert that two products with identical flash peaks are formed via energetically identical pathways. In terms of bond breaking and formation this statement is equivalent to saying that they proceed via identical chemical intermediates. In the case that the normal flash desorption analysis [4] allows a definite reaction order to be determined, the order can be used to quantify the molecularity of the rate-determining reaction step. The molecular identity of reactants and products then lead to the deduction of the intermediates involved. The latter identification can be greatly assisted by the use of isotopic substitution.

2. Experimental

The interaction of ethanol with Ag(110) and Cu(110) was studied by TPRS and conducted in the stainless steel ultrahigh vacuum system previously described [7]. The UHV chamber was equipped with a PHI four-grid LEED Auger optics, an argon ion bombardment gun and a UTI-100C quadrupole mass spectrometer. The single crystal samples could be cooled to about 180 K by heat conduction through a copper braid attached to a liquid nitrogen cooled copper tube. The samples were heated from the rear by radiation from a tungsten filament; a heating rate of 13 K s⁻¹ was employed for the copper sample and about 15 K s⁻¹ for the silver sample. The samples were not present simultaneously in the UHV chamber since only one sample

could be accommodated. Deuterated ethanol, $\text{CH}_3\text{CH}_2\text{OD}(99\% \text{D})$, was obtained from Stohler Isotope Chemicals and introduced onto the front face of the crystal surfaces through a stainless steel dosing syringe backed by the ethanol vapor pressure obtained above liquid $\text{CH}_3\text{CH}_2\text{OD}$ at 195 K. The purification procedure was the same as that previously described for methanol [5]. The mass spectrometer signal for each product formed during the flash decomposition experiment was directly proportional to the desorption rate because of the high pumping speed of the system. The peak temperatures were always reproducible to within ± 5 K.

The products observed in this study were identified by carefully comparing their observed cracking patterns in the mass spectrometer with those tabulated in the literature and those determined in the present UHV system. Once the product was identified, the ionized parent molecule, i.e. $m/e = 47$ for $\text{CH}_3\text{CH}_2\text{OD}$, $m/e = 2$ for H_2 , etc., was used to monitor the product. The only exceptions were $\text{CH}_3\text{CH}_2\text{OH}$ where $m/e = 45$ was monitored in order to avoid overlap with the $\text{CH}_3\text{CH}_2\text{OD}$ $m/e = 46$ signal, and CH_3CHO where $m/e = 29$ was monitored because of the substantially larger acetaldehyde signal produced. In addition, the C_2H_4 and D_2O spectra had to be corrected for cracking contributions of other molecules. A more extensive discussion on product identification by mass spectrometry will be found in the Appendix.

The (110) orientations of the copper and silver single crystals were verified by low energy electron diffraction (LEED) and surface cleanliness was achieved at the beginning of each experiment by Argon ion sputtering. Auger electron spectroscopy verified that typical surface contaminants such as carbon and sulfur were not present on the copper and silver surfaces prior to an experiment. Although the Ag(110) surface was found to remain free of contaminants during the course of a day's experimentation, the Cu(110) sample exhibited about 5–10% of a surface carbon monolayer at the end of the day. For an extensive discussion of AES analysis of the Cu(110) and Ag(110) surfaces see the previous studies on the oxidation of methanol on these same crystals [5,6].

Enriched oxygen (99% $^{18}\text{O}_2$) was purchased from Bio Rad Laboratories and was introduced into the background of the UHV chamber through a variable leak valve. Oxygen background pressures of 10^{-8} – 10^{-6} Torr were employed during the adsorption of oxygen, and the silver and copper samples were always maintained at 295 ± 10 K. Under these conditions the initial sticking probabilities of molecular oxygen on the Cu(110) and Ag(110) surfaces were found to be $\approx 5 \times 10^{-2}$ and $\approx 1 \times 10^{-3}$, respectively [5,8]. The surface coverages of oxygen on Cu(110) were previously determined by AES for several different oxygen exposures and are tabulated in table 1 [5] (a Langmuir is defined as 1×10^{-6} Torr of oxygen exposure). Since the sticking probability of oxygen on Ag(110) was much lower than on Cu(110), it was increased by a factor of 3–4 by switching on the ionizer of the mass spectrometer and facing the front side of the crystal toward the ionizer. The surface concentrations of oxygen on the silver sample were estimated from knowledge of the initial sticking probability of oxygen on the Ag(110) surface and are

Table 1

The surface coverages of oxygen on Cu(110) as determined from AES. See ref. [5] for details.

Oxygen exposure (Langmuirs)	Surface coverage of oxygen (fraction of monolayer)
0.2	0.04
0.45	0.05
1.2	0.14
2.0	0.22
5.0	0.40

Table 2

The surface coverages of oxygen on Ag(110). See ref. [6] for details.

Oxygen exposure with MS on (Langmuirs)	Surface coverage of oxygen (fraction of monolayer)
30	0.06
60	0.19
90	0.34
180	0.61
300	0.85
500	0.99

tabulated in table 2 [6]. For a more detailed discussion on the calibration of the surface coverages and sticking probabilities of oxygen on the Cu(110) and Ag(110) surfaces see the previous studies on the oxidation of methanol on these same samples [5,6]. The bulk of the experiments on the oxidation of ethanol on Cu(110) and Ag(110) were conducted on surfaces containing approximately 10–20% oxygen.

3. Results for ethanol oxidation on Ag(110)

In order to provide the reader with a guide to the extensive results section the major results will be summarized first. The behavior of each product species will then be considered in turn. The product distribution following adsorption of $\text{CH}_3\text{CH}_2\text{OD}$ to near saturation at ≈ 180 K on a Ag(110) preoxidized surface is shown in fig. 1. Two temperature regimes were observed in which products were evolved. $\text{CH}_3\text{CH}_2\text{OD}$, CH_3CHO , C_2H_4 , H_2 and D_2O (deuterated water *not* enriched with ^{18}O) desorbed at 220 ± 10 K. The simultaneous evolution of these molecules suggested that they had a common rate-limiting step on the Ag(110) surface. Furthermore, they formed only after the formation of CH_3CHO at 275 K suggesting their dependence on the presence of adsorbed CH_3CHO . At higher temperatures $\text{CH}_3\text{CH}_2\text{OD}$, CH_3CHO , $\text{CH}_3\text{CH}_2\text{OH}$ and H_2 desorbed simultaneously at 275 ± 10 K,

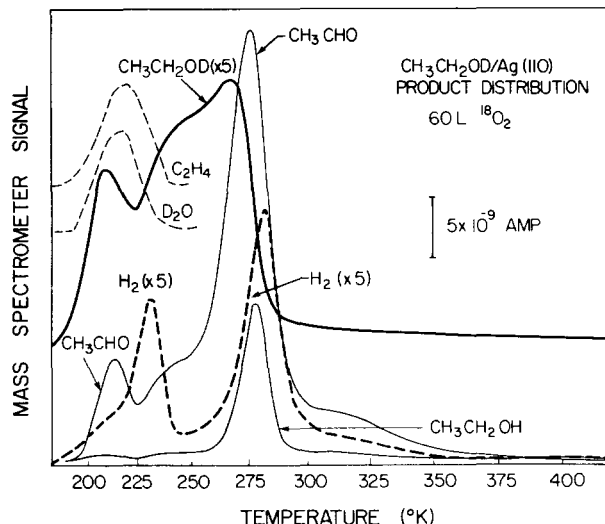


Fig. 1. Temperature programmed spectrum following $\text{CH}_3\text{CH}_2\text{OD}$ adsorption at 180 K on a Ag(110) surface that was predosed with $^{18}\text{O}_2$ at 295 ± 10 K. The oxygen exposure applied was 60 L with the MS on; the $\text{CH}_3\text{CH}_2\text{OD}$ exposure was 150 s. These curves are uncorrected for detection sensitivities.

and CH_3CHO , H_2 and $\text{CH}_3\text{CH}_2\text{OH}$ desorbed again to a much smaller extent at 320 ± 5 K. Note that $\text{CH}_3\text{CH}_2\text{OH}$ was formed even though $\text{CH}_3\text{CH}_2\text{OD}$ was initially adsorbed on the silver surface. These results suggest immediately two major reaction pathways existed on the surface.

The deuterium atom was selectively removed from $\text{CH}_3\text{CH}_2\text{OD}$ during adsorption, because D_2^{18}O was the first product to desorb and was *displaced from the Ag(110) surface during the adsorption process*. The D_2^{18}O signal was thus monitored *during the adsorption of $\text{CH}_3\text{CH}_2\text{OD}$ at 180 K* on the partially oxidized Ag(110) substrate. The front face of the (110) oriented silver crystal was preferentially oxidized by dissociating the oxygen in the mass spectrometer. As a blank calibration the backside of the Ag(110) sample was first exposed to $\text{CH}_3\text{CH}_2\text{OD}$ from the doser and almost no D_2^{18}O was formed, but when the sample was rotated to expose the oxidized face of the Ag(110) crystal a large D_2^{18}O signal was observed. The D_2^{18}O signal initially increased as a function of time, and then decayed to zero when the ^{18}O atoms on the Ag(110) surface were consumed. The HD^{18}O and H_2^{18}O signals were also monitored in the same manner, but only trace amounts were formed. This experiment verified that D_2^{18}O was selectively formed and displaced from the partially oxidized Ag(110) surface by other species during the adsorption of $\text{CH}_3\text{CH}_2\text{OD}$ at 180 K to saturation coverage.

Trace amounts of HD^{18}O and H_2^{18}O were also observed during the adsorption process, but D_2^{18}O accounted for greater than 90% of the water displaced from the

Ag(110) surface. No HD or D₂ was observed to desorb throughout the entire temperature range because *all of the deuterium atoms were involved in the formation of water*. No other ethanol oxidation products were observed: in particular, carbon dioxide, carbon monoxide, methane, ethyl acetate and diethyl ether were absent from the spectrum.

The integrated mass spectrometer signals of CH₃CHO, CH₃CH₂OD and C₂H₄ are presented in fig. 2 as a function of ethanol exposure on a Ag(110) surface exposed to 60 L ¹⁸O₂ with the MS on. The first product to form at low ethanol exposures was acetaldehyde. A delay was observed in the evolution of ethanol from the silver surface; almost no ethanol desorbed following a 13 s exposure. A longer delay was observed for the production of C₂H₄; almost no C₂H₄ was observed following a 25 s exposure. These results suggested that the non-dissociative adsorption of CH₃CH₂OD on the partially oxidized silver surface depended on a sufficient concentration of the surface intermediate responsible for acetaldehyde formation and that ethylene formation depended on a sufficient concentration of surface ethoxide and ethanol. This intermediate was deduced to be CH₃CH₂O from the observations that (1) D₂¹⁸O was desorbed from the surface upon adsorption of CH₃CH₂OD on the ¹⁸O covered surface (little HD¹⁸O was formed) and (2) CH₃CHO and H₂ were formed simultaneously in a reaction limited step subsequent to D₂¹⁸O formation. The formation of the ethoxide intermediate from CH₃CH₂OD was found to be quite sensitive to the concentration of preadsorbed oxygen as shown in figs. 9 and 10. This behavior was quite consistent with that observed for methoxide formation on Cu(110) [5] and Ag(110) [6].

A more detailed discussion for the results for each product now follows.

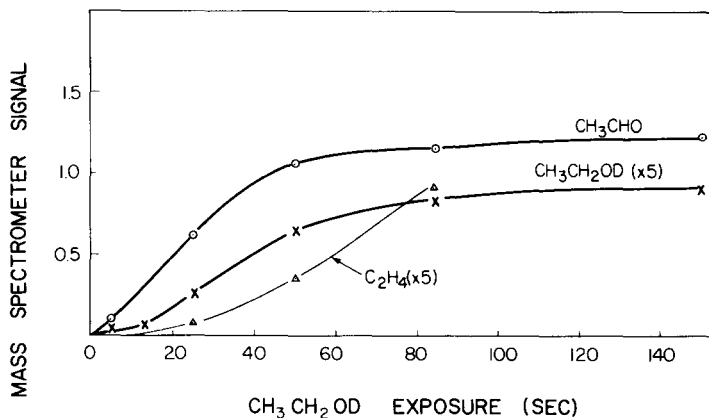


Fig. 2. The integrated CH₃CHO, CH₃CH₂OD, and C₂H₄ mass spectrometer signals as a function of ethanol exposure. The Ag(110) surface was always preoxidized at 295 ± 10 K by 60 L ¹⁸O₂ with the MS on and CH₃CH₂OD was adsorbed at 180 K. These curves are uncorrected for detection sensitivities. The different detection sensitivities do not alter the relative magnitudes of the products.

3.1. Water/ $\text{CH}_3\text{CH}_2\text{OD}$

The production of D_2^{18}O during the flash from the oxidation of $\text{CH}_3\text{CH}_2\text{OD}$ is shown in fig. 3. The D_2^{18}O peak temperatures shifted to lower temperatures with increasing coverage, but at high coverages almost no D_2^{18}O was observed during the flash; the D_2^{18}O signal exhibited a maximum as a function of $\text{CH}_3\text{CH}_2\text{OD}$ exposure. This behavior suggested that the D_2^{18}O -substrate bond was weakened with increasing coverage and that D_2^{18}O was displaced by other intermediates from the Ag(110) surface.

Subsequent to low exposures of $\text{CH}_3\text{CH}_2\text{OD}$ (less than 25 s) some H_2^{18}O and HD^{18}O were produced only during the flash because not all of the surface ^{18}O was consumed during adsorption at 180 K by reaction to form D_2^{18}O . The absence of the products H_2^{18}O and HD^{18}O for ethanol exposure greater than 25 s was not due to displacement from the silver surface, since substantial H_2^{18}O and HD^{18}O signals were not detected during adsorption at 180 K; it was due to selective titration of $^{18}\text{O}_{(a)}$ by D atoms released upon $\text{CH}_3\text{CH}_2\text{OD}$ adsorption. The HD^{18}O formed on the unsaturated surfaces resulted from the reaction of ^{18}OD , formed during the adsorption of $\text{CH}_3\text{CH}_2\text{OD}$ at 180 K and hydrogen atoms released by surface intermediates during the flash (see fig. 1). The H_2^{18}O signal similarly resulted from the reaction of hydrogen atoms released during the temperature programmed reaction and excess ^{18}O atoms present on the Ag(110) surface. Maximum H_2^{18}O and HD^{18}O production was observed for EtOD exposure of 5–13 s above which a rapid decrease to near zero was observed.

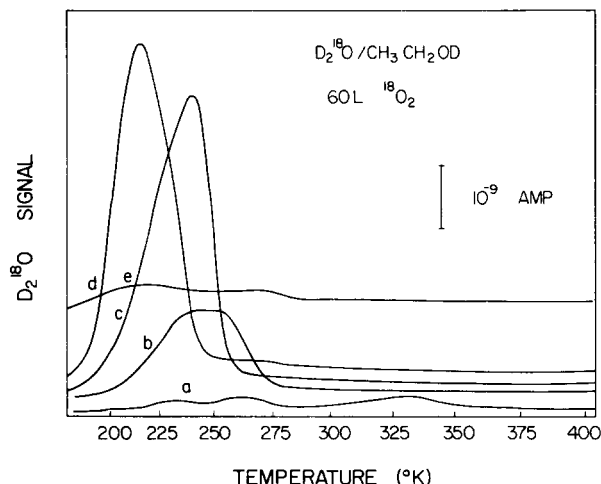


Fig. 3. The D_2^{18}O desorption spectra subsequent to the oxidation of $\text{CH}_3\text{CH}_2\text{OD}$ on Ag(110). The $\text{CH}_3\text{CH}_2\text{OD}$ was adsorbed at 180 K on a Ag(110) surface that was predeposited with $^{18}\text{O}_2$ at 295 ± 10 K. The oxygen exposure applied was 60 L with the MS on. The $\text{CH}_3\text{CH}_2\text{OD}$ exposures were (a) 1 s, (b) 5 s, (c) 13 s, (d) 25 s and (e) 75 s.

The formation of D_2O/CH_3CH_2OD (deuterated water *not* enriched with ^{18}O) was only observed following ethanol exposures greater than 25 s. Since the production of D_2O/CH_3CH_2OD and C_2H_4/CH_3CH_2OD exhibited the same characteristics they will be discussed simultaneously below.

3.2. CH_3CHO/CH_3CH_2OD

The CH_3CHO spectra from the partially oxidized Ag(110) surface are shown in fig. 4 as a function of CH_3CH_2OD exposure at 180 K. The β_3 peak developed first and was the most prominent CH_3CHO peak at all coverages; the $CH_3CHO(\beta_3)/CH_3CH_2OD$ will thus be taken as representative of acetaldehyde production from ethanol on Ag(110). The invariance of the CH_3CHO/CH_3CH_2OD peak temperatures with coverage demonstrated that the production of CH_3CHO occurred via a first-order process on the Ag(110) surface. The $CH_3CHO(\beta_1)/CH_3CH_2OD$ peak was only observed subsequent to ethanol exposures greater than 25 s and exhibited the same peak temperature and delay with ethanol exposure as C_2H_4/CH_3CH_2OD , see fig. 2. The kinetic parameters for the formation of CH_3CHO from CH_3CH_2OD could not be accurately determined because of the overlap of the different CH_3CHO peaks.

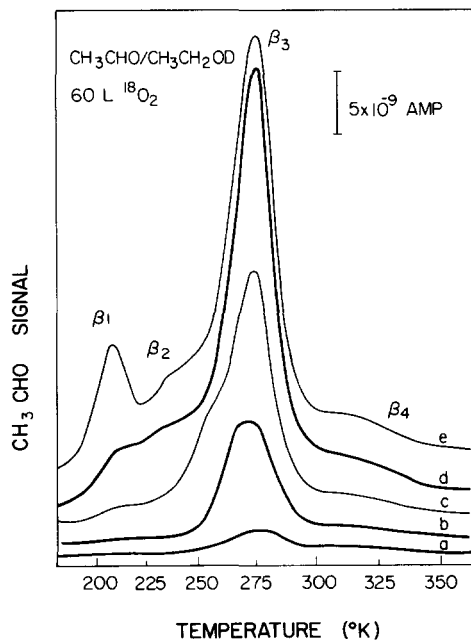


Fig. 4. The CH_3CHO temperature programmed spectra as a function of CH_3CH_2OD exposure. The Ag(110) surface was always preexposed by 60 L $^{18}O_2$, with the MS on, at 295 ± 10 K prior to adsorption of CH_3CH_2OD at 180 K. The CH_3CH_2OD exposures were (a) 5 s, (b) 13 s, (c) 25 s, (d) 50 s and (e) 85 s.

The $\text{CH}_3\text{CHO}/\text{CH}_3\text{CH}_2\text{OD}$ peak temperatures corresponded to the $\text{CH}_3\text{CH}_2\text{OH}/\text{CH}_3\text{CH}_2\text{OD}$ peak temperatures and acetaldehyde formation will be discussed below in conjunction with $\text{CH}_3\text{CH}_2\text{OH}$ formation.

3.3. $\text{CH}_3\text{CH}_2\text{OH}/\text{CH}_3\text{CH}_2\text{OD}$

The $\text{CH}_3\text{CH}_2\text{OH}$ temperature programmed reaction spectra subsequent to the adsorption of $\text{CH}_3\text{CH}_2\text{OD}$ on the partially oxidized silver substrate are presented in fig. 5. The $\text{CH}_3\text{CH}_2\text{OH}$ β_3 and β_4 peak temperatures were essentially the same as the corresponding H_2 and CH_3CHO peaks and suggested that these three products originated from the same surface intermediate. Since the deuterium atom was removed from $\text{CH}_3\text{CH}_2\text{OD}$ to form D_2^{18}O upon adsorption and $\text{CH}_3\text{CH}_2\text{OH}$, CH_3CHO and H_2 were formed simultaneously, this surface intermediate was ethoxide. The surface reactions responsible for these three products were

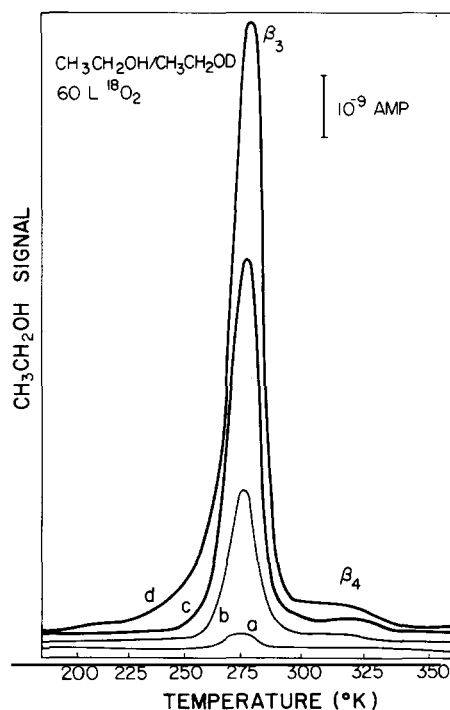


Fig. 5. The $\text{CH}_3\text{CH}_2\text{OH}$ desorption spectra subsequent to the adsorption of $\text{CH}_3\text{CH}_2\text{OD}$ at 180 K on a partially oxidized Ag(110) surface. The surface was predosed with 60 L $^{18}\text{O}_2$ at 295 ± 10 K while the MS was on. The $\text{CH}_3\text{CH}_2\text{OD}$ exposures were (a) 5 s, (b) 13 s, (c) 25 s and (d) 50 s.



Analogous reactions were previously observed with surface methoxide when methanol was adsorbed on partially oxidized Cu(110) [5] and Ag(110) [6]. A substantial $\text{CH}_3\text{CH}_2\text{OH}(\beta_1)/\text{CH}_3\text{CH}_2\text{OD}$ peak was not observed.

3.4. $\text{CH}_3\text{CH}_2\text{OD}/\text{CH}_3\text{CH}_2\text{OD}$

The desorption spectra of $\text{CH}_3\text{CH}_2\text{OD}$ are shown in fig. 6 as a function of coverage. The absence of D_2 and D_2^{18}O from the spectrum following high ethanol exposures (see fig. 1) revealed that $\text{CH}_3\text{CH}_2\text{OD}$ evolution from the Ag(110) surface resulted from ethanol that did *not* dissociate upon adsorption. The $\text{CH}_3\text{CH}_2\text{OD}/\text{CH}_3\text{CH}_2\text{OD}$ spectra showed peaks close to the $\text{CH}_3\text{CHO}/\text{CH}_3\text{CH}_2\text{OD}$ peaks (see fig. 4). The $\text{CH}_3\text{CH}_2\text{OD}$ peaks filled the same way as the CH_3CHO peaks as a function of $\text{CH}_3\text{CH}_2\text{OD}$ exposure, but the $\text{CH}_3\text{CH}_2\text{OD}$ peak temperatures were consistently 5–10 K lower. These results and the previous observation that $\text{CH}_3\text{CH}_2\text{OD}$

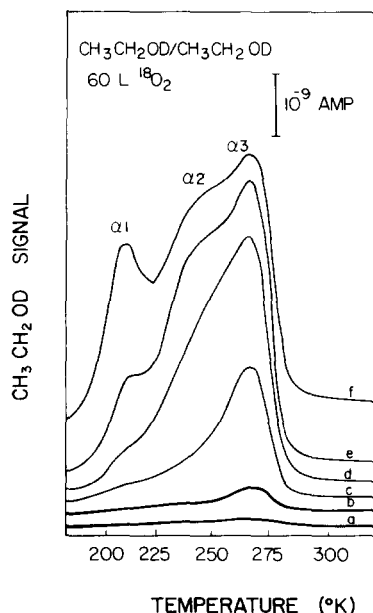


Fig. 6. The $\text{CH}_3\text{CH}_2\text{OD}$ desorption spectra subsequent to the adsorption of $\text{CH}_3\text{CH}_2\text{OD}$ at 180 K on a Ag(110) surface predosed with $^{18}\text{O}_2$ at 295 ± 10 K. 60 L of oxygen was applied with the MS on. The $\text{CH}_3\text{CH}_2\text{OD}$ exposures were (a) 5 s, (b) 13 s, (c) 25 s, (d) 50 s, (e) 85 s and (f) 150 s.

only desorbed following a sufficient concentration of the surface ethoxide suggested that $\text{CH}_3\text{CH}_2\text{OD}$ was stabilized on the Ag(110) surface by surface ethoxide. The $\text{CH}_3\text{CH}_2\text{OD}(\alpha_1)/\text{CH}_3\text{CH}_2\text{OD}$ peak was only observed following ethanol exposure greater than 25 s and exhibited the same peak temperature and delay with ethanol exposures as $\text{C}_2\text{H}_4/\text{CH}_3\text{CH}_2\text{OD}$ (see fig. 2).

3.5. C_2H_4 and $\text{D}_2\text{O}/\text{CH}_3\text{CH}_2\text{OD}$

The C_2H_4 temperature programmed reaction spectra are shown in fig. 7 as a function of $\text{CH}_3\text{CH}_2\text{OD}$ exposure. C_2H_4 was only produced following $\text{CH}_3\text{CH}_2\text{OD}$ exposures greater than 25 s. The invariance of the $\text{C}_2\text{H}_4/\text{CH}_3\text{CH}_2\text{OD}$ peak temperature with coverage revealed that ethylene was produced by a first-order surface process. The $\text{D}_2\text{O}/\text{CH}_3\text{CH}_2\text{OD}$ spectra were identical to the $\text{C}_2\text{H}_4/\text{CH}_3\text{CH}_2\text{OD}$ spectra and D_2O was also only observed following ethanol exposures greater than 25 s. The simultaneous evolution of C_2H_4 , D_2O , $\text{H}_2(\beta_1)$, $\text{CH}_3\text{CHO}(\beta_1)$, $\text{CH}_3\text{CH}_2\text{OD}(\beta_1)$ indicated that ethylene originated from the interaction of two adsorbed $\text{CH}_3\text{CH}_2\text{OD}$ molecules. The formation of D_2O and the absence of D_2 required the formation of $\text{CH}_3\text{CH}_2\text{OD}_2$ with subsequent decomposition according to

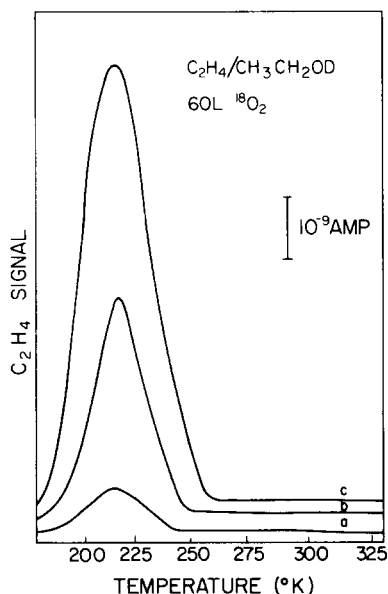
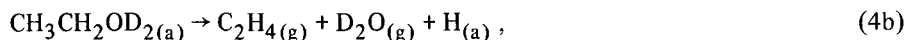


Fig. 7. The desorption of C_2H_4 subsequent to the adsorption of $\text{CH}_3\text{CH}_2\text{OD}$ on a partially oxidized Ag(110) surface. The ethylene spectra were corrected for cracking contributions of $\text{CH}_3\text{CH}_2\text{OD}$, $\text{CH}_3\text{CH}_2\text{OH}$ and CH_3CHO . The Ag(110) sample was oxidized by 60 L $^{18}\text{O}_2$ with the MS on at 295 ± 10 K and $\text{CH}_3\text{CH}_2\text{OD}$ was adsorbed on the partially oxidized surface at 180 K. The $\text{CH}_3\text{CH}_2\text{OD}$ exposures were (a) 25 s, (b) 50 s and (c) 85 s.



The surface intermediate $\text{CH}_3\text{CH}_2\text{OD}_2$ was formed from the direct interaction of two $\text{CH}_3\text{CH}_2\text{OD}$ molecules because D_2 , HD , HD^{18}O and D_2^{18}O were not observed during the flash for ethanol exposures greater than 25 s, that is, deuterium atoms were not released to the surface since *no* D_2 was observed to form, though H_2 readily desorbed. The exact mechanism by which the two ethanol molecules initially interacted is not known.

The stability of the $\text{CH}_3\text{CH}_2\text{OD}_2_{(a)}$ intermediate cannot be accessed from the results. The independence of the position of C_2H_4 , D_2O and $\text{H}_2(\beta_1)$ peaks with coverage indicate that either step (4b) was rate-determining or that the $\text{CH}_3\text{CH}_2\text{OD}$ species were adsorbed contiguously so that step (4a) was pseudo first order.

3.6. $\text{H}_2/\text{CH}_3\text{CH}_2\text{OD}$

The H_2 spectra from the oxidation of $\text{CH}_3\text{CH}_2\text{OD}$ on the silver substrate are presented in fig. 8. The $\text{H}_2(\beta_1)/\text{CH}_3\text{CH}_2\text{OD}$ peak only became prominent following a 25 s exposure of ethanol and was a composite of two hydrogen peaks. In the vicin-

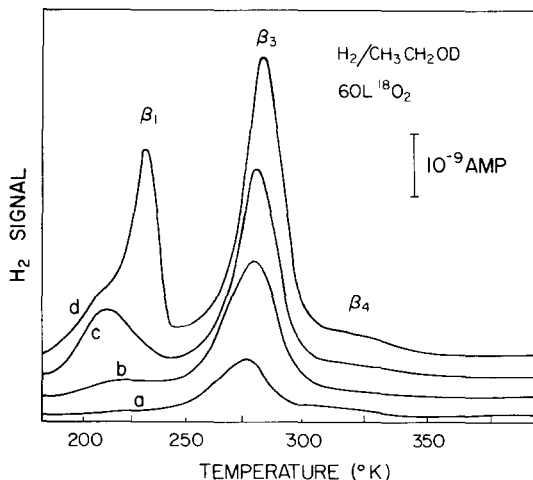


Fig. 8. H_2 production subsequent to $\text{CH}_3\text{CH}_2\text{OD}$ decomposition on a partially oxidized Ag(110) surface. The Ag(110) surface was oxidized by 60 L $^{18}\text{O}_2$ with the MS on at 295 ± 10 K prior to the adsorption of $\text{CH}_3\text{CH}_2\text{OD}$ at 180 K. The $\text{CH}_3\text{CH}_2\text{OD}$ exposures were (a) 5 s, (b) 13 s, (c) 25 s and (d) 85 s.

ity of 225 K hydrogen was formed both from the decomposition of surface ethoxide to acetaldehyde, step (1), and the decomposition of the surface intermediate $\text{CH}_3\text{CH}_2\text{OD}_2$, step (4). The $\text{H}_2(\beta_1)/\text{CH}_3\text{CH}_2\text{OD}$ peak temperature was approximately 5–7 K higher than the C_2H_4 and D_2O peaks because the hydrogen recombination process, step (5), was not instantaneous at 225 K on the Ag(110) surface [6]. The $\text{H}_2(\beta_3)/\text{CH}_3\text{CH}_2\text{OD}$ and $\text{H}_2(\beta_4)/\text{CH}_3\text{CH}_2\text{OD}$ peak temperatures were also about 5–7 K higher than the $\text{CH}_3\text{CHO}(\beta_3)/\text{CH}_3\text{CH}_2\text{OD}$ and $\text{CH}_3\text{CHO}(\beta_4)/\text{CH}_3\text{CH}_2\text{OD}$ peaks and originated from the decomposition of surface ethoxide, step (1). Hydrogen was thus formed on the Ag(110) surface during the oxidation of ethanol from the decomposition of two different surface intermediates: $\text{CH}_3\text{CH}_2\text{O}$ and $\text{CH}_3\text{CH}_2\text{OD}_2$.

3.7. Oxygen variation studies

In order to examine the function of oxygen upon the oxidation of ethanol on silver the oxygen exposure was varied from 0–90 L while a constant ethanol exposure of 150 s was maintained. The pronounced effect of the surface concentration of oxygen upon CH_3CHO formation and desorption of $\text{CH}_3\text{CH}_2\text{OD}$ is shown in fig. 9. Only trace amounts of CH_3CHO and $\text{CH}_3\text{CH}_2\text{OD}$ were observed on the oxygen-free silver surface, and the signals increased dramatically with oxygen exposure. The small amount of ethanol that chemisorbed on the oxygen-free silver surface may have been partially due to the adsorption of background oxygen from the UHV system. These results demonstrated that very little ethanol chemisorbed on an oxygen-free silver surface, and that ethanol interacted with surface oxygen atoms during the adsorption process since surface oxygen enhanced the sticking probability of ethanol on silver. The selective formation of D_2^{18}O during the adsorption of

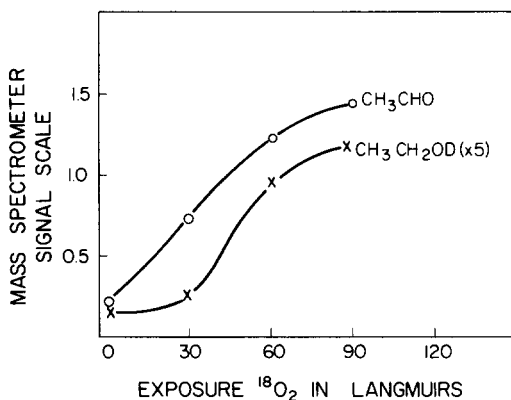


Fig. 9. The influence of oxygen exposure upon the production of CH_3CHO and $\text{CH}_3\text{CH}_2\text{OD}$ following a 150 s exposure of $\text{CH}_3\text{CH}_2\text{OD}$ at 180 K. The Ag(110) surface was always oxidized at 295 ± 10 K with the MS on. These curves are uncorrected for detection sensitivities.

$\text{CH}_3\text{CH}_2\text{OD}$ revealed that the hydroxyl end of the ethanol molecule interacted with the surface oxygen atom during the adsorption process.

The influence of surface oxygen upon the CH_3CHO temperature programmed reaction spectra is shown in fig. 10. Very little acetaldehyde was produced on the oxygen-free Ag(110) surface, and the amount of acetaldehyde produced increased dramatically with increasing oxygen coverage. The various acetaldehyde binding states on the Ag(110) surface were not affected by the different concentrations of surface oxygen because the peak temperatures were constant with oxygen exposure and no new peaks were observed. The binding states of the various other products were also not affected by the amount of oxygen on the surface. This result indicated that over the range of surface oxygen concentration investigated the Ag(110) surface did not reconstruct.

The total amount of undissociated $\text{CH}_3\text{CH}_2\text{OD}$ adsorbed on the Ag(110) surface also increased substantially with increasing oxygen exposure. The enhanced adsorption was most likely due to the stabilization of $\text{CH}_3\text{CH}_2\text{OD}$ on the silver surface through bonding via surface ethoxide since the oxygen-free Ag(110) surface only

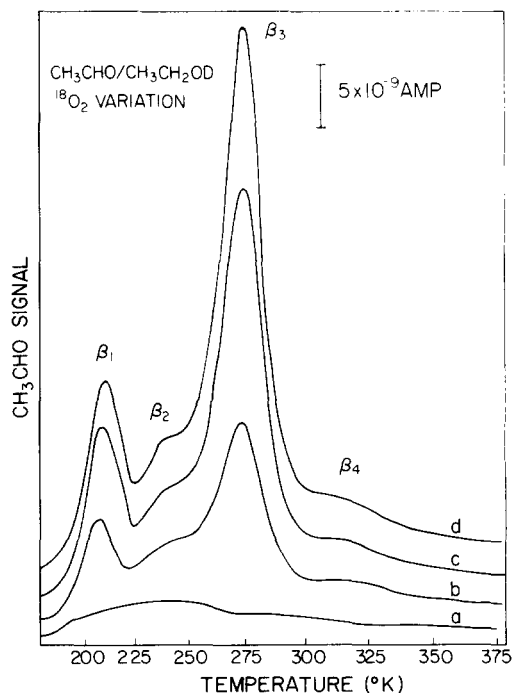


Fig. 10. The influence of oxygen exposure upon the CH_3CHO spectra. The Ag(110) surface was oxidized at 295 ± 10 K with the MS on and was given a 150 s dose of $\text{CH}_3\text{CH}_2\text{OD}$ at 180 K. The oxygen exposures were (a) 0 L, (b) 30 L, (c) 60 L and (d) 90 L.

Table 3

Summary of the results observed for the oxidation of $\text{CH}_3\text{CH}_2\text{OD}$ on Ag(110). The Ag(110) surface was oxidized at 295 ± 10 K and exposed to $\text{CH}_3\text{CH}_2\text{OD}$ at 180 K. E^* is the activation energy calculated for a single first-order rate-limiting step from T_p assuming $\log_{10}\nu = 13$.

State	T_p (K)	E^* (kcal/mole)
$\text{C}_2\text{H}_4/\text{CH}_3\text{CH}_2\text{OD}$	220 ± 3	12.8
$\text{D}_2\text{O}/\text{CH}_3\text{CH}_2\text{OD}$	220 ± 3	12.8
$\text{CH}_3\text{CH}_2\text{OD}(\alpha_1)/\text{CH}_3\text{CH}_2\text{OD}$	210	12.2
$\text{CH}_3\text{CH}_2\text{OD}(\alpha_2)/\text{CH}_3\text{CH}_2\text{OD}$	240 ± 5	14.0
$\text{CH}_3\text{CH}_2\text{OD}(\alpha_3)/\text{CH}_3\text{CH}_2\text{OD}$	265	15.5
$\text{CH}_3\text{CHO}(\beta_1)/\text{CH}_3\text{CH}_2\text{OD}$	215	12.5
$\text{CH}_3\text{CHO}(\beta_2)/\text{CH}_3\text{CH}_2\text{OD}$	240 ± 5	14.0
$\text{CH}_3\text{CHO}(\beta_3)/\text{CH}_3\text{CH}_2\text{OD}$	273	16.0
$\text{CH}_3\text{CHO}(\beta_4)/\text{CH}_3\text{CH}_2\text{OD}$	320 ± 5	18.8
$\text{H}_2(\beta_1)/\text{CH}_3\text{CH}_2\text{OD}$	230	13.4
$\text{H}_2(\beta_3)/\text{CH}_3\text{CH}_2\text{OD}$	283	16.6
$\text{H}_2(\beta_4)/\text{CH}_3\text{CH}_2\text{OD}$	320 ± 5	18.8
$\text{CH}_3\text{CH}_2\text{OH}(\beta_3)/\text{CH}_3\text{CH}_2\text{OD}$	276	16.1
$\text{CH}_3\text{CH}_2\text{OH}(\beta_4)/\text{CH}_3\text{CH}_2\text{OD}$	320 ± 5	18.8

adsorbed a small amount of ethanol and the $\text{CH}_3\text{CH}_2\text{OD}/\text{CH}_3\text{CH}_2\text{OD}$ spectra were very similar to the $\text{CH}_3\text{CHO}/\text{CH}_3\text{CH}_2\text{OD}$ spectra. The desorption of $\text{CH}_3\text{CH}_2\text{OD}$ exhibited a delay with ethanol exposure (see fig. 2) because initially $\text{CH}_3\text{CH}_2\text{OD}$ was oxidized to $\text{CH}_3\text{CH}_2\text{O}$, and only after a sufficient concentration of $\text{CH}_3\text{CH}_2\text{O}$ was present on the surface was it possible for ethanol to adsorb non-dissociatively.

3.8. Summary of results

The results observed for the oxidation of $\text{CH}_3\text{CH}_2\text{OD}$ on the silver (110) surface are tabulated above in table 3. The notation $A(\alpha)/B$ refers to the α state or desorption peak for gas A following adsorption of gas B. E^* was calculated from the peak temperature of each state assuming a first-order reaction step with frequency factor $\nu = 10^{13} \text{ s}^{-1}$ in order to provide a relative value of the activation energy. All of the reaction steps observed in this study exhibited first-order kinetics.

4. Results for ethanol oxidation on Cu(110)

The interaction of ethanol with the (110) oriented copper single crystal surface was *qualitatively* examined in order to compare the characteristics of this system with the above results on the Ag(110) surface. The ethanol temperature programmed

reaction spectrum from a copper surface *not* predosed with $^{18}\text{O}_2$ † is shown in fig. 11 subsequent to a 150 s exposure of $\text{CH}_3\text{CH}_2\text{OD}$. The ethanol spectrum from the Cu(110) surface was very similar to that reported for the Ag(110) surface, see fig. 1. The species $\text{CH}_3\text{CH}_2\text{OD}$, CH_3CHO , D_2O and C_2H_4 also desorbed simultaneously at 225 ± 5 K from Cu(110). The major $\text{CH}_3\text{CH}_2\text{OD}$ binding state on Cu(110) at 282 K, also appeared at a slightly lower temperature than the major CH_3CHO peak; CH_3CHO and $\text{CH}_3\text{CH}_2\text{OH}$ desorbed simultaneously at 316 K. Hydrogen, hydrogen deuteride and deuterium (the HD and D_2 spectra are not presented in fig. 11) were the last products to desorb from Cu(110) because they were desorption-limited on this surface [5]. The similar temperature programmed reaction spectra of ethanol from Cu(110) and Ag(110), figs. 1 and 11, clearly demonstrated that the intermediates formed subsequent to the adsorption of $\text{CH}_3\text{CH}_2\text{OD}$ were the same on both surfaces.

The simultaneous desorption of C_2H_4 , D_2O , CH_3CHO and $\text{CH}_3\text{CH}_2\text{OD}$ at 225 ± 5 K from Cu(110) and the same species, with the addition of H_2 , from the partially oxidized Ag(110) at 220 ± 10 K implied that the same surface intermediate

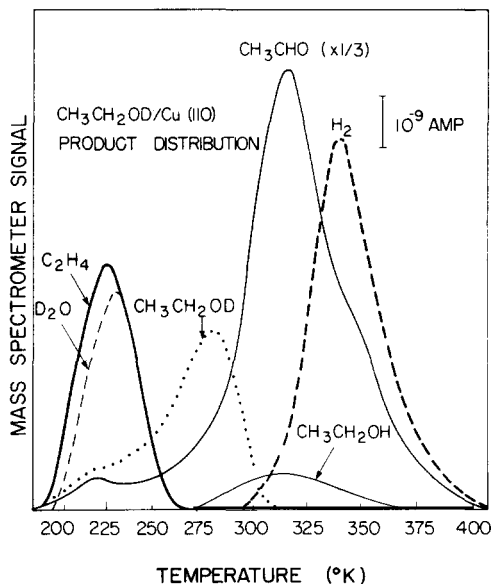


Fig. 11. The temperature programmed reaction spectrum obtained following $\text{CH}_3\text{CH}_2\text{OD}$ adsorption at 180 K on an oxygen-free Cu(110) surface. These curves are uncorrected for detection sensitivities.

† The deficiency of D_2 evolved at 350 K in the product spectrum indicated that some $^{16}\text{O}_2$ was inadvertently dosed with $\text{CH}_3\text{CH}_2\text{OD}$ through the doser. Due to the higher sticking probability of O_2 on Cu relative to Ag this effect was more difficult to control.

$\text{CH}_3\text{CH}_2\text{OD}_2$ was also produced on the Cu(110) surface from the interaction of two $\text{CH}_3\text{CH}_2\text{OD}$ molecules. Similarly at higher surface temperatures, 316 K, CH_3CHO and $\text{CH}_3\text{CH}_2\text{OH}$ desorbed simultaneously indicating that they also originated from the decomposition of an ethoxide intermediate (see reaction steps (1) to (3)). The acetaldehyde production exhibited first-order kinetics since its peak temperature was independent of coverage for more than a ten-fold increase in amplitude. Hydrogen peaks were absent from the spectrum below about 340 K because hydrogen was desorption-limited on Cu(110) [5]. The ratio of H_2/HD observed at 340 K was about three and only trace amounts of D_2 were observed. The production of HD and D_2 revealed that in the absence of oxygen the Cu(110) surface could, to a limited extent, form ethoxide upon adsorption of $\text{CH}_3\text{CH}_2\text{OD}$.

4.1. Oxygen variation studies

The influence of surface oxygen upon the interaction of $\text{CH}_3\text{CH}_2\text{OD}$ with the Cu(110) surface was briefly examined. For the same exposure of $\text{CH}_3\text{CH}_2\text{OD}$, 150 s, the magnitudes of the acetaldehyde and H_2 peaks increased by a factor of 2.5 when the copper surface was predosed with 1 L $^{18}\text{O}_2$; the same amount of $\text{C}_2\text{H}_4/\text{CH}_3\text{CH}_2\text{OD}$ was produced on the undosed and the partially oxidized copper surfaces. These results demonstrated that ethanol also interacted with the surface oxygen atoms during adsorption on Cu(110) and thereby enhanced the formation of ethoxide. The surface concentration of oxygen employed did not affect the CH_3CHO , H_2 and C_2H_4 peak positions.

Table 4

Summary of the results observed for the decomposition of $\text{CH}_3\text{CH}_2\text{OD}$ on Cu(110). $\text{CH}_3\text{CH}_2\text{OD}$ was adsorbed at 180 K on an oxygen-free Cu(110) surface.

State	T_p (K)	E (kcal/mole)	ν (s^{-1})	E^* a) (kcal/mole)
$\text{C}_2\text{H}_4/\text{CH}_3\text{CH}_2\text{OD}$	225	—	—	13.1
$\text{D}_2\text{O}/\text{CH}_3\text{CH}_2\text{OD}$	228	—	—	13.3
$\text{CH}_3\text{CH}_2\text{OD}(\alpha_1)/\text{CH}_3\text{CH}_2\text{OD}$	220	—	—	12.8
$\text{CH}_3\text{CH}_2\text{OD}(\alpha_3)/\text{CH}_3\text{CH}_2\text{OD}$	282	—	—	16.6
$\text{CH}_3\text{CHO}(\beta_1)/\text{CH}_3\text{CH}_2\text{OD}$	220	—	—	12.8
$\text{CH}_3\text{CHO}(\beta_3)/\text{CH}_3\text{CH}_2\text{OD}$	316	20.4 ± 1.0 b)	$5.0 \pm 4.0 \times 10^{13}$ b)	18.7
$\text{CH}_3\text{CHO}(\beta_4)/\text{CH}_3\text{CH}_2\text{OD}$	350	—	—	20.7
$\text{CH}_3\text{CH}_2\text{OH}/\text{CH}_3\text{CH}_2\text{OD}$	316	—	—	18.7
$\text{D}_2 + \text{HD} + \text{H}_2/\text{CH}_3\text{CH}_2\text{OD}$	340	—	—	—

a) E^* is the activation energy calculated for a single first-order rate-limiting step from T_p assuming $\log_{10}\nu = 13$.

b) The kinetic parameters were calculated by the method of heating rate variation [4].

Table 5

Summary of the results observed for the oxidation of CH₃OH on Cu(110). The Cu(110) surface was oxidized at 295 ± 10 K and exposed to CH₃OH at 180 K.

State	T_p (K)	E (kcal/mole)	ν (s ⁻¹)	E^* a) (kcal/mole)
CH ₃ OH(α_1)/CH ₃ OH	200 ± 5	–	–	12.1
CH ₃ OH(α_2)/CH ₃ OH	245 ± 5	–	–	14.8
CH ₃ OH(α_3)/CH ₃ OH	275	–	–	16.7
CH ₃ OH(β_1)/CH ₃ OH	330 ± 5	–	–	20.1
CH ₃ OH(β_2)/CH ₃ OH	365	–	–	22.4
CH ₃ OH(β_3)/CH ₃ OH	390	–	–	23.9
H ₂ CO(β_2)/CH ₃ OH	365	22.1 ± 0.1 b)	5.2 ± 1.6 × 10 ¹² b)	22.4
H ₂ CO(β_3)/CH ₃ OH	392	19.3 ± 0.4 c)	1.5 ± 0.7 × 10 ¹⁰ c)	24.0
H ₂ (β_1)/CH ₃ OH	325 ± 5	–	–	19.8
H ₂ (β_2)/CH ₃ OH	370	22.0 b)	3.6 × 10 ¹² b)	22.6
H ₂ (β_3)/CH ₃ OH	390	–	–	23.9
H ₂ (γ)/CH ₃ OH	470	30.9 ± 0.2 b)	8.0 ± 2.0 × 10 ¹³ b)	29.0
C ¹⁶ O ¹⁸ O/CH ₃ OH	470	30.9 ± 0.2 b)	8.0 ± 2.0 × 10 ¹³ b)	29.0
H ₂ ¹⁸ O(δ_1)/CH ₃ OH	238	–	–	14.3
H ₂ ¹⁸ O(δ_2)/CH ₃ OH	290	–	–	17.6
H ₂ ¹⁸ O(δ_3)/CH ₃ OH	320	–	–	19.5
H ₂ ¹⁸ O(γ)/CH ₃ OH	470	30.9 ± 0.2 b)	8.0 ± 2.0 × 10 ¹³ b)	29.0

a) E^* is the activation energy calculated for a single first-order rate-limiting step from T_p assuming $\log_{10}\nu = 13$.

b) The kinetic parameters were calculated by the method of heating rate variation [4].

c) The kinetic parameters were calculated by plotting $\ln(R/C)$ versus $1/T$ [4].

4.2. Summary of results

The results observed for the interaction of CH₃CH₂OD with the oxygen-free copper(110) surface are tabulated above in table 4. The flash decomposition peaks were labeled following the procedure outlined in table 3. The previous results obtained for the oxidation of methanol on copper(110) and Ag(110) are presented in tables 5 and 6 for comparison. All of the reaction steps observed, except H₂/CH₃CH₂OD on Cu(110), exhibited first-order kinetics.

5. Discussion

The results of the preceding section led to the following conclusions about the oxidation of CH₃CH₂OD on Ag(110):

Table 6

Summary of the results observed for the oxidation of CH₃OD on Ag(110). The Ag(110) surface was oxidized at 295 ± 10 K and exposed to CH₃OD at 180 K.

State	T_p (K)	E (kcal/mole)	ν (s ⁻¹)	E^* a) (kcal/mole)
HCOOCH ₃ (α_1)/CH ₃ OD	250	13.1 ± 0.6 ^{b)}	4.5 ± 3.5 × 10 ¹¹ b)	14.6
HCOOCH ₃ (α_2)/CH ₃ OD	280 ± 3	13.3 ± 0.4 ^{c)}	2.5 ± 1.5 × 10 ¹⁰ c)	16.3
CH ₃ OH(α_1)/CH ₃ OD	252	—	—	14.7
CH ₃ OH(α_2)/CH ₃ OD	280 ± 3	—	—	16.3
CH ₃ OH(β_2)/CH ₃ OD	300	—	—	18.6
CH ₃ OH(β_3)/CH ₃ OD	340	—	—	20.0
H ₂ CO(β_1)/CH ₃ OD	250	—	—	14.6
H ₂ CO(β_2)/CH ₃ OD	300	—	—	17.6
H ₂ CO(β_3)/CH ₃ OD	340 ± 10	—	—	20.0
H ₂ (β_1)/CH ₃ OD	250	—	—	14.6
H ₂ (β_2)/CH ₃ OD	312	—	—	18.3
H ₂ (β_3)/CH ₃ OD	350	—	—	20.6
H ₂ (γ)/CH ₃ OD	402	22.2 ± 0.5 ^{b)}	1.1 ± 0.7 × 10 ¹² b)	23.8
C ¹⁶ O ¹⁸ O/CH ₃ OD	402	22.2 ± 0.5 ^{b)}	1.1 ± 0.7 × 10 ¹² b)	23.8
DCOOCH ₃ /CH ₃ OD, D ₂ CO	273	14.0 ± 0.5 ^{b)}	2.4 ± 2.0 × 10 ¹¹ b)	16.0

a) E^* is the activation energy calculated for a single first-order rate-limiting step from T_p assuming $\log_{10}\nu = 13$.

b) The kinetic parameters were calculated by plotting $\ln(R/C)$ versus $1/T$ [4].

c) The kinetic parameters were calculated from isothermal plots [4].

(1) Surface oxygen enhanced both the dissociative and non-dissociative chemisorption of CH₃CH₂OD on the silver surface, and only trace amounts of ethanol chemisorbed on the oxygen-free Ag(110) surface.

(2) The hydroxyl end of the CH₃CH₂OD molecule interacted with surface ¹⁸O atoms during the dissociative adsorption process to form adsorbed CH₃CH₂O and D₂¹⁸O.

(3) D₂¹⁸O was displaced by other surface intermediates from the Ag(110) surface into the gas phase following ethanol exposures greater than 25 s during adsorption at 180 K.

(4) H₂¹⁸O and HD¹⁸O were also observed to desorb during the flash from the silver substrate when the ratio of adsorbed ¹⁸O to adsorbed CH₃CH₂O was high.

(5) The simultaneous appearance of CH₃CH₂OH, CH₃CHO and H₂ resulted from the reaction of an adsorbed CH₃CH₂O intermediate.

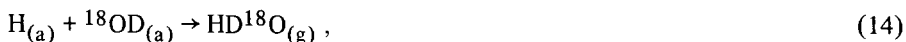
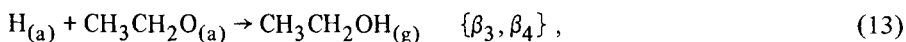
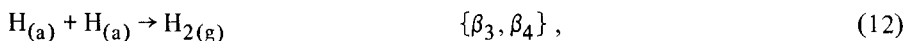
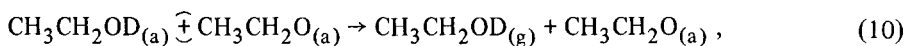
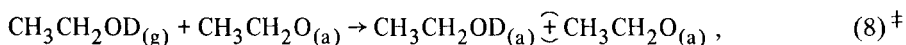
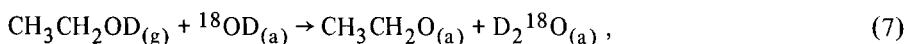
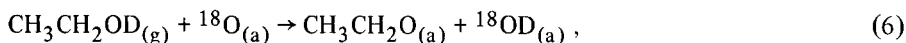
(6) C₂H₄, D₂O and H₂(β_1)/CH₃CH₂OD were only produced following ethanol exposures greater than 25 s and originated from the decomposition of the surface intermediate CH₃CH₂OD₂.

(7) The interaction of two $\text{CH}_3\text{CH}_2\text{OD}$ molecules during the adsorption process resulted in the formation of adsorbed $\text{CH}_3\text{CH}_2\text{OD}_2$ and CH_3CHO .

(8) The adsorption of undissociated $\text{CH}_3\text{CH}_2\text{OD}$ was enhanced through bonding via surface ethoxide.

Many of the above observations for the oxidation of ethanol on Ag(110) are very similar to that previously reported for methanol oxidation on this catalyst surface [6].

The oxidation mechanism following low exposures of ethanol on Ag(110), when the ratio of $^{18}\text{O}/\text{CH}_3\text{CH}_2\text{O}$ on the surface was high, occurred as follows:



The above mechanism took place on the Ag(110) surface when all of the surface oxygen atoms were not selectively titrated to $\text{D}_2{}^{18}\text{O}$ upon $\text{CH}_3\text{CH}_2\text{OD}$ adsorption. Subsequent to ethanol exposures greater than 25 s the surface intermediates $\text{CH}_3\text{CH}_2\text{OD}_2$ and $\text{CH}_3\text{CH}_2\text{O}$ were formed during adsorption from the interaction of two ethanol molecules. The ethoxide subsequently decomposed to $\text{CH}_3\text{CHO}(\beta_1)/\text{CH}_3\text{CH}_2\text{OD}$ and $\text{H}_2(\beta_1)/\text{CH}_3\text{CH}_2\text{OD}$, same as reaction step (11), and $\text{CH}_3\text{CH}_2\text{OD}_2$ decomposed to C_2H_4 , D_2O and hydrogen, see reaction steps (4) and (5). The intermediate $\text{CH}_3\text{CH}_2\text{OD}_2$ was only formed following high exposures of ethanol because at low exposures most of the adsorbed ethanol was converted to ethoxide and the formation of adsorbed $\text{CH}_3\text{CH}_2\text{OD}_2$ required the presence of undissociated ethanol on the surface. The reaction mechanism thus demonstrates that the selectivity to-

[‡] The notation $\hat{\oplus}$ signifies induced adsorption.

wards the formation of ethylene or acetaldehyde was a function of the ratio of oxygen to ethoxide present on the Ag(110) surface.

The above discussion indicated that the two most important surface intermediates during the oxidation of ethanol on Ag(110) were $\text{CH}_3\text{CH}_2\text{O}$ and $\text{CH}_3\text{CH}_2\text{OD}_2$ since they were responsible for the production of the major reaction products: acetaldehyde and ethylene. The ethoxide was the *most abundant surface intermediate* on the Ag(110) surface even following high ethanol exposures because much more acetaldehyde than ethylene was produced. Other investigators have also reported that when alcohols are chemisorbed on oxide catalysts surface alkoxide species are often formed [9]. A surface intermediate analogous to $\text{CH}_3\text{CH}_2\text{OD}_2$ has been proposed when ethanol is dehydrated over a catalyst surface containing acidic sites [10]. Thus the two surface intermediates formed by the adsorption of ethanol on the partially oxidized Ag(110) surface have previously been postulated in other catalytic investigations, but the present study revealed that they are also *stable* surface intermediates under UHV conditions and that they are formed on metallic surfaces with low oxygen coverage.

The oxidation of $\text{CH}_3\text{CH}_2\text{OD}$ on the Cu(110) and the Ag(110) surfaces exhibited many similar characteristics. Ethanol was oxidized to surface ethoxide and water upon adsorption, and the ethoxide subsequently decomposed to acetaldehyde and hydrogen on both surfaces. C_2H_4 and D_2O were also formed on both substrates at approximately 220 K following high exposures of ethanol and originated from the decomposition of the intermediate $\text{CH}_3\text{CH}_2\text{OD}_2$. Surface oxygen atoms enhanced the formation of ethoxide from ethanol on the Cu(110) and Ag(110) surfaces. These observations indicated that the same mechanisms, reaction steps (4) to (13), were operative on the partially oxidized Cu(110) and Ag(110) surfaces.

The relative reaction behavior for Ag and Cu observed is in general agreement with other comparisons available between silver and copper. The sticking probability for the dissociative adsorption of formic acid was much higher for Cu(110) than Ag(110), and the surface formate subsequently formed was stable to higher surface temperatures on Cu(110) [11,12]. The initial sticking probability of oxygen was also more than an order of magnitude higher on Cu(110) than on Ag(110); oxygen desorbed from the silver substrate at elevated temperatures, but not from the copper substrate at comparable surface coverages [5,6,8]. The Cu(110) surface also formed stronger bonds with other adsorbates because (1) D_2^{18}O was not displaced during the adsorption process from Cu(110), (2) H_2 desorbed at approximately 340 K from Cu(110) [5] and 225 K from Ag(110) [6], and (3) the ethoxide intermediate exhibited greater stability on Cu(110) than on Ag(110). The major acetaldehyde peak from the decomposition of surface ethoxide occurred at 316 K on Cu(110) and 273 K on Ag(110). Such a decrease in the peak temperature corresponds to about 3 kcal/mole decrease in activation energy for the decomposition of the ethoxide if the pre-exponential factor is assumed constant at 10^{13} s^{-1} . The above comparisons reveal that the sticking probabilities for the dissociative adsorption of various molecules were greater on Cu(110) than Ag(110), and that the rate

constants for the subsequent decomposition of the surface intermediates were larger on Ag(110) than Cu(110).

The oxidation of CH₃OD on the Cu(110) and Ag(110) catalysts [5,6] also exhibited many similar characteristics and proceeded by reaction mechanisms analogous to the oxidation of CH₃CH₂OD. Methanol was oxidized to CH₃O and D₂¹⁸O upon adsorption, and methoxide was the most abundant surface intermediate on both substrates. The subsequent decomposition of the methoxide intermediate was responsible for the formation of H₂CO and hydrogen. On the Ag(110) surface adsorbed formaldehyde also interacted with surface methoxide to yield methyl formate. The methoxide was stable until about 300 K on Ag(110) and 365 K on Cu(110) at low coverages. Such a decrease in the peak temperature corresponds to about 5 kcal/mole decrease in the activation energy for the decomposition of the methoxide on silver relative to copper if the pre-exponential factor was assumed constant at 10¹³ s⁻¹. The above observations further substantiated that alkoxides were more stable on a copper than a silver substrate, and that silver catalysts were thus more reactive than copper catalysts for the decomposition of alkoxides to aldehydes or ketones.

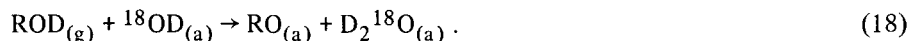
The relative stability of the ethoxides was less than the methoxides on the Cu(110) and Ag(110) surfaces since the ethoxides decomposed at lower temperatures than the methoxides on both surfaces. Bradley [13] also reported the same order of stabilities for zirconium alkoxides Zr(OCH₃)₄ > Zr(OCH₂CH₃)₄ > Zr(OCH(CH₃)₂)₄. The stability of the surface alkoxides correlates with the strength of the α-hydrogen C–H bond [14] in ethanol (about 88 kcal/mole) and methanol (about 92 kcal/mole) because their rate of decomposition is related to the strength of this carbon–hydrogen bond. Furthermore the energy involved in the disruption of the RO–H bond is the same for both alcohols [15], and thus the rates for formation of alkoxides



should be approximately the same for methanol and ethanol on a particular catalyst. Since the *relative* oxidation rates of both alcohols on the *same catalyst* depend only on the stability of the alkoxide intermediates, the rate of oxidation of ethanol to acetaldehyde should generally be greater than the oxidation rate of methanol to formaldehyde. The oxidation of methanol and ethanol to their corresponding aldehydes was examined over an iron-molybdenum catalyst [16] in the temperature range 180–240°C, and the reactivity of ethanol was found to be higher by one order of magnitude. The oxidation of methanol and ethanol were similarly compared over a thorium-molybdate catalyst [17] in the temperature range 220–280°C, and ethanol was again found to oxidize more rapidly than methanol. These investigators also reported that the activation energies for the oxidation of ethanol were approximately 3–6 kcal/mole lower than the corresponding methanol oxidations. The present study showed that the activation energy for the decomposition of the ethoxide was about 2 kcal/mole lower on Ag(110) and about 4 kcal/mole lower on Cu(110)

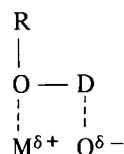
than for the decomposition of the corresponding methoxide if the pre-exponential factor for both reactions was assumed to be 10^{13} s^{-1} . Note that the differences in activation energies between methanol and ethanol during oxidation over the above catalysts were approximately the same as the difference in the α -hydrogen C–H bond strength between methanol and ethanol.

The present investigations of alcohol oxidation on Cu(110) and Ag(110) revealed that the surface oxygen atoms were the active sites for alkoxide formation. The surface oxygen atoms behaved effectively as basic sites since they selectively removed the hydroxyl hydrogens from the alcohols to form alkoxides



Other catalytic studies of alcohols on various oxide catalysts [18,19] and acid/base bifunctional catalysts [20–22] also indicate that basic sites were responsible for the dehydrogenation of alcohols. The active sites for the dehydrogenation of isopropanol were attributed to basic O^{2-} for MgO, CaO and SrO [18] and O_2^- or HOO^- on the surface of MnO_2 [19]. Basic sites were similarly concluded to be the active sites for the production of acetaldehyde from ethanol on silica-magnesia [20] and the formation of surface ethoxide from ethanol on silica-alumina [21]. An extensive examination of the dehydrogenation of several different alcohols over alkaline earth silicate acid/base bifunctional catalysts also concluded that dehydrogenation of alcohols occurred on basic sites [22].

Many of these investigators also suggested that the active sites consisted of a Lewis acid site–basic site pair, i.e., a metal ion and an adjacent basic oxygen ion. The results of the present studies on Cu(110) and Ag(110) also support the concept of a *dual site mechanism* for the dissociative adsorption of alcohols



in which the metal ion serves as an adsorption site for the alkoxide and the oxygen site for the adsorption of the hydroxyl hydrogen. The present investigations demonstrated that the presence of oxygen on the metal surfaces enhanced the adsorption of alcohols. Apparently zero valent copper and silver have little affinity for alcohols and the surface oxygen created metal sites with a positive valence promoting the adsorption of the alcohol via interaction of the electron donating oxygen lone pair. The $\text{M}^{\delta+}\text{O}^{\delta-}$ dual site thus produced a more efficient splitting of the O–D bond in ROD.

6. Conclusion

The results of this study clearly demonstrated that the interaction of alcohols with partially oxidized Ag(110) and Cu(110) surfaces formed surface alkoxides and water upon adsorption. The surface oxygen atoms enhanced alkoxide formation, and a dual site $M^{\delta+}O^{\delta-}$ was suggested for the dissociative adsorption of alcohols on these surfaces. The ethoxides were less stable than the methoxides on both surfaces, and Ag(110) was more active than Cu(110) for the dehydrogenation of the alkoxides to aldehydes. The formaldehyde yield was determined by the competitive formation of CO_2 , and the acetaldehyde yield was similarly determined by the production of C_2H_4 . This work illustrates further the applicability of UHV kinetic studies to more complex reaction systems.

Acknowledgement

The authors gratefully acknowledge the support of the National Science Foundation (NSF-ENG-74-15509) throughout the course of this work.

Appendix

The mass peaks (m/e) chosen to monitor CH_3CH_2OD , CH_3CH_2OH and CH_3CHO were 47, 45 and 29, respectively. The $CH_3CHO(29)$ peak was corrected for cracking contributions from CH_3CH_2OD and CH_3CH_2OH [23].

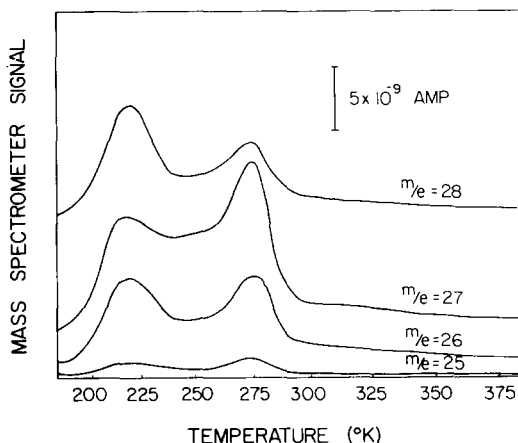


Fig. 12. The $m/e = 28, 27, 26$ and 25 signals obtained subsequent to the adsorption of CH_3CH_2OD at 180 K on a Ag(110) surface that was preposed by 60 L $^{18}O_2$ with the MS on at 295 ± 10 K.

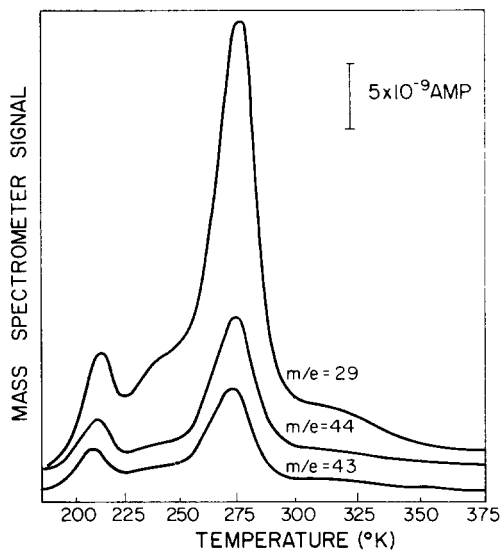


Fig. 13. The $m/e = 29, 44$ and 43 signals obtained subsequent to the adsorption of $\text{CH}_3\text{CH}_2\text{OD}$ at 180 K on a $\text{Ag}(110)$ surface that was preadsorbed by $60\text{ L }^{18}\text{O}_2$ with the MS on at $295 \pm 10\text{ K}$.

Ethylene, C_2H_4 ($m/e = 28$), was isolated as a major reaction product by its four major ionization peaks: $m/e = 28, 27, 26$ and 25 [24]. The $m/e = 28, 27, 26$ and 25 signals from the oxidation of $\text{CH}_3\text{CH}_2\text{OD}$ on $\text{Ag}(110)$ are presented in fig. 12. The peaks at about 273 K were due to the fragmentation of $\text{CH}_3\text{CH}_2\text{OD}$, $\text{CH}_3\text{CH}_2\text{OH}$ and CH_3CHO in the mass spectrometer, but the magnitude of the peaks at about 220 K were much greater than the contributions of these species and verified that substantial ethylene was produced at about 220 K . Furthermore, the $m/e = 28, 27, 26$ and 25 signals at about 220 K were corrected for the contributions of the various

Table 7
The mass spectrum of $\text{CH}_3\text{CH}_2\text{OD}$ and $\text{CH}_3\text{CH}_2\text{OH}$ a).

m/e	$\text{CH}_3\text{CH}_2\text{OD}$		m/e	$\text{CH}_3\text{CH}_2\text{OH}$	
	Identity abundance			Identity abundance	
32	CH_2OD	100	31	CH_2OH	100
46	$\text{C}_2\text{H}_4\text{OD}$	35	45	$\text{C}_2\text{H}_4\text{OH}$	34
27	C_2H_3	23	27	C_2H_3	22
29	$\text{HCO}, \text{C}_2\text{H}_5$	17	29	$\text{HCO}, \text{C}_2\text{H}_5$	19
47	$\text{C}_2\text{H}_5\text{OD}$	15	46	$\text{C}_2\text{H}_5\text{OH}$	15

a) See ref. [23].

reaction products and the relative ratios of the corrected signals agreed well with the fragmentation patterns of ethylene reported in the literature [24]. The ethylene spectra of fig. 7 were corrected for the cracking contributions of $\text{CH}_3\text{CH}_2\text{OD}$, $\text{CH}_3\text{CH}_2\text{OH}$ and CH_3CHO .

The various isotopes of water were monitored by recording the $m/e = 22$ (D_2^{18}O), the $m/e = 21$ (HD^{18}O) and the $m/e = 20$ (H_2^{18}O and D_2^{16}O) signals. The H_2^{18}O and D_2^{16}O signals were distinguished by simultaneously examining $m/e = 19$ ($^{18}\text{OH}^+$) and $m/e = 18$ ($^{16}\text{OD}^+$) [24]. Since D_2^{16}O was only produced following ethanol exposures greater than 25 s and H_2^{18}O was only formed following ethanol exposures less than 25 s their respective signals did not coincide and these two forms of water were thus distinguishable. Following high exposures of ethanol the D_2^{16}O signal had to be corrected for cracking contributions from $\text{CH}_3\text{CH}_2\text{OD}$ [23], the D_2^{16}O signals in figs. 1 and 11 were corrected for these contributions.

References

- [1] C.L. Thomas, *Catalytic Processes and Proven Catalysts* (Academic Press, New York, 1970) p. 208.
- [2] J.F. Walker, *Formaldehyde* (Reinhold, New York, 1964) p. 1.
- [3] C.L. Thomas, *Catalytic Processes and Proven Catalysts* (Academic Press, New York, 1970) p. 49.
- [4] J.L. Falconer and R.J. Madix, *Surface Sci.* 48 (1975) 393; *J. Catalysis* 48 (1977) 262.
- [5] I.E. Wachs and R.J. Madix, *J. Catalysis*, submitted for publication.
- [6] I.E. Wachs and R.J. Madix, *Surface Sci.*, to be submitted for publication.
- [7] J. McCarty, J. Falconer and R.J. Madix, *J. Catalysis* 30 (1973) 235.
- [8] H.A. Engelhardt and D. Menzel, *Surface Sci.* 57 (1976) 591.
- [9] C.L. Kibby and W.K. Hall, *J. Catalysis* 31 (1973) 65.
- [10] H. Pines and J. Manassen, *Advan. Catalysis* 16 (1966) 49.
- [11] I.E. Wachs, D.H.S. Ying and R.J. Madix, to be published.
- [12] S.K. Miller and R.J. Madix, to be published.
- [13] D.C. Bradley, *Progr. Inorg. Chem.* 2 (1960) 303.
- [14] V.I. Vedenev, L.V. Gurvich, V.N. Kondratev, V.A. Frankevich and E.Y. Frankevich, *Energy of Disruption of Chemical Bonds* (Izd. Akad. Nauk SSSR, Moscow, 1962) p. 71.
- [15] C.T. Mortimer, *Reaction Heats and Bond Strengths* (Pergamon, New York, 1962) p. 136.
- [16] N.P. Evmenko and Ya.B. Gorokhovatskii, *Kinet. Catal.* 11 (1970) 104.
- [17] V. Srihari and D.S. Viswanath, *J. Catalysis* 43 (1976) 43.
- [18] Z.G. Szabo, B. Jover and R. Ohmacht, *J. Catalysis* 39 (1975) 225.
- [19] S. Hasegawa, K. Yasuda, T. Mase and T. Kawaguchi, *J. Catalysis* 46 (1977) 125.
- [20] H. Niiyama, S. Morii and E. Echigoya, *Bull. Chem. Soc. Japan* 45 (1972) 655.
- [21] F.F. Roca, L. DeMourgues and Y. Trambouze, *J. Catalysis* 14 (1969) 107.
- [22] H. Niiyama and E. Echigoya, *Bull. Chem. Soc. Japan* 44 (1971) 1739.
- [23] L.W. Sieck, F.P. Abramson and J.H. Futrell, *J. Chem. Phys.* 45 (1966) 2859.
- [24] E. Stenhagen, S. Abrahamson and F.W. McLafferty, eds., *Atlas of Mass Spectral Data*, Vol. 1 (Interscience, New York, 1969).